An Experimental Comparison of Evaporating and Non-evaporating Sprays in a Simple Turbulent Jet Flow

S. H. Stårner and A. R. Masri

School of Aerospace, Mechanical and Mechatronic Engineering
University of Sydney, NSW 2006

ABSTRACT

This paper presents detailed measurements in turbulent jets lightly loaded with evaporating (acetone) and non-evaporating (mineral turpentine) spray. This work forms part of a larger program to study spray jets and flames in a simple, well defined geometry with the objective of providing the necessary platform for developing and validating predictive tools for such flows. Phase-Doppler anemometry is applied and issues of flow-field, droplet dispersion, size distribution and evaporation rates are addressed. The sprays have less than four percent mass loading to suppress effects of agglomeration and other particle interactions.
The total liquid-phase flow is found to be well conserved for the non-evaporating case, whilst the acetone case reveals substantial bulk evaporation. The smallest size class exhibits a marked rise in flow at downstream locations, and a corresponding modification of the acetone size distribution is observed. Turbulent diffusion of the smallest droplets is close to that of the gas phase, whilst the largest droplets are found to be confined to trajectories with low dispersion, positive slip velocity and high ratio of axial to radial rms turbulence velocity, reflecting weak interaction with the gas phase turbulence. There is no substantial difference in the dispersion of the evaporating and non-evaporating sprays. The non-evaporating (mineral turps) droplet probability density function (pdf) changes only modestly with downstream distance. The acetone spray pdf, however, shows shifting of peak values towards smaller sizes, with a distinctly bimodal shape developing.

1. Introduction

Numerical modelling of single phase jet flows can be said to have reached a state of maturity, in large part owing to the wealth of experimental studies now available on slender shear flows such as the round jet, against which sub-models can be thoroughly tested. The same cannot be said for two-phase flows, firstly due to the extra complexity of the coupled dynamics of the phases, and secondly because of the lack of reliable experimental data which is essential for the development and validation of physical sub-models. The ideal laboratory flow would be experimentally tractable as well as numerically simple enough to enable isolation of the effects of turbulence, evaporation, droplet interactions and chemical reaction (as in spray flames). Many industrially relevant sprays have been investigated in detail, but such flows usually involve recirculation, high velocity and poor optical access, and are not well suited to the study of the basic mechanisms. It is against this background that the present

work is undertaken: following many studies of simple round jet in a co-flowing stream, with and without reaction [1], these experiments have been extended by entraining a droplet cloud into the jet, well upstream of the exit into the co-flow. By this means, a flow is set up that has simple, well-known fluid mechanics, moderate velocity and droplet loading, and well-defined initial conditions. Previous papers in this series report on very fine sprays created by air-blast generated droplets in a nebulizer [2,3]. Here we use an ultrasonic generator which produces larger droplets, more akin to what is seen in industrial applications. Recent work by others in similar geometries focuses on particular aspects, such as very dense sprays [4], time of flight statistics of monodisperse sprays [5] and evaporation and coalescence [6].

Unlike conventional cone-type spray generators which tend to disperse the large droplets to the periphery, this spray has initially uniform axial flow direction for all sizes, thus simplifying the study of dispersion and stratification due to turbulent transport. Importantly, the low mass loading enables accurate flux measurements to be made for all size classes throughout the jet. In McDonnell and Samuelsen's thorough study [7] of pressure-atomized sprays, the difficulty in measuring droplet mass flow rates in conventional nozzles is highlighted: the recorded droplet mass flow increases continuously up to 100 mm from the nozzle due to the high upstream rejection rate. This is indeed the case in most reported cases. To compensate for this near-exit loss, Ferrand et al. [4] obtain the flow rates per size class by coupling measured mean LIF intensity with PDA output, and using the assumption that the rejection rate is independent of size class, so that the recorded size distribution near the exit is argued to be valid also for the rejected droplet fraction. The relatively low mass loading used here makes such assumptions superfluous: the mass flow is shown here to be conserved throughout for the non-evaporating case. Thus, for the evaporating case, this lends firm support to the contention that droplet fluxes and evaporation rates are accurately obtained.

One of the main contributions of this paper is to provide a quantitative understanding of the differences between non-evaporating and evaporating lightly loaded spray jets. An initial step in the development of reliable numerical tools for sprays is to ascertain that processes such as spray dispersion, turbulence-droplet interactions and droplet size distributions are properly accounted for in non-evaporating and evaporating flows. The data provided within, forms a necessary platform for such validations.

2. Experimental

The spray nozzle assembly shown in Fig. 1 is mounted in a 3 m/s co-flowing air stream with less than 2 per cent turbulence intensity. The main fuel tube is 200 mm long and has a10.0mm

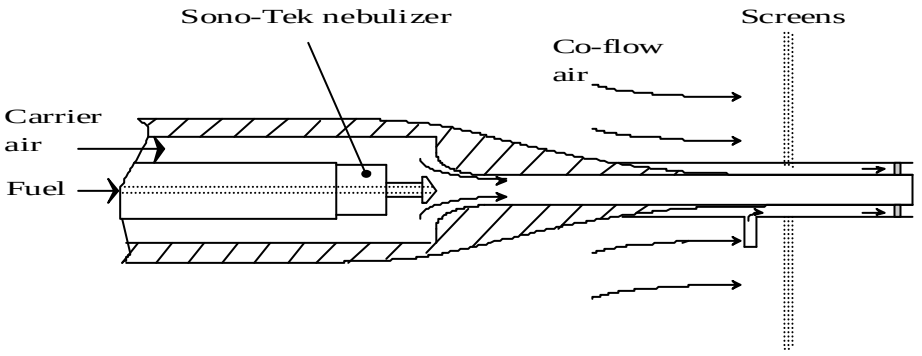

Figure 1. Nozzle configuration.

inner diameter, D. The annulus surrounding the nozzle end is a pilot flame holder which is necessary for flame stabilization but is not used here. Instead, air is supplied through the pilot annulus at the same bulk velocity as in the co-flow, to avoid recirculation at the jet exit. There is no back-flow of liquid into the bottom of the nozzle. Ultrasonically generated droplets with Sauter mean diameter around 40 microns and near zero momentum are entrained into the air carrier stream (Reynolds number 13,000), resulting initially in a wide range of slip velocities due to differential acceleration from rest in the nozzle tube. Flow rates are measured by rotameters.

Mineral turpentine ('turps'), a non-toxic and inexpensive fluid, is used as the non-evaporative liquid. It has a boiling range of 150-190 ^{o}C at atmospheric pressure, and consists mainly of $C_{10}H_{16}$. To emphasize the evaporation rate, acetone (also used for LIF studies in this series of experiments [2]) is used for the evaporating spray. Its boiling point is 56.5 ^{o}C at atmospheric pressure. The injected flow rates, measured by stop-watch, are 4.85 and 8.80 ml/min for turps and acetone, respectively. The droplet flow rates at the jet exit, obtained by integrating measured droplet fluxes across the jet, are 4.1 and 3.6 ml/min for turps and acetone respectively. Thus, the higher evaporation rate of acetone in the nozzle tube has been compensated for by a higher injection rate, to obtain similar droplet flow rates at the jet exit.

The phase Doppler anemometer (Aerometrics model 3200) is arranged in 45 degree forward scattering, with 300 mm receiver focal length and 3 micron fringe spacing. A 7W argon-ion laser feeds the fiber-optics assembly. The power in each beam at the measurement volume is 50-100 mW. Photomultiplier voltages are set at 350-400 V. Two components of velocity are recorded. Software correction is made for the lower visibility of small droplets at the edge of the measurement volume. Correction is also made for velocity bias. It should be noted that as only the jet stream is 'seeded' with droplets, the recorded velocities approximate to turbulent zone averages.

Size and velocity data are recorded in five radial traverses of the jet, up to 30 nozzle diameters from the jet exit (shown normalized as x/D, where x is the axial distance from the nozzle exit and D is the nozzle diameter). To maximize the quality of the flux measurements, only the axial velocity is measured together with the size data; this is found to yield the highest size validation percentage. Two-channel velocity and size measurements are made as a separate operation to obtain radial velocity and shear stress data, the size data being used only to separate the velocity data into size classes.

It is important that photomultiplier voltages, detection thresholds and beam intensities be maintained constant throughout the length of the jet. It would be tempting, in order to maximize the local PDA validation rate, to alter these parameters at large x/D since the *average* system saturation rate falls with concentration. However, this would alter the visibility of small droplets and hence bias the size distribution relative to upstream results. Settings are thus in effect determined by the saturation constraints at the jet exit.

3. Results and discussion

One of the striking differences in the overall behaviour of these two spray jets is best demonstrated by comparing the development of the droplet size distributions shown in Figure 2. The probability density functions (pdf's) at the jet exit are seen to be quite similar, both on the axis and in mid shear layer, i.e., where the axial velocity gradient peaks. It should be noted that at the jet exit the shear layer is very thin, so that the measurement location shown in Figure 2 is within 0.5 mm of the nozzle radius. However, with increasing axial

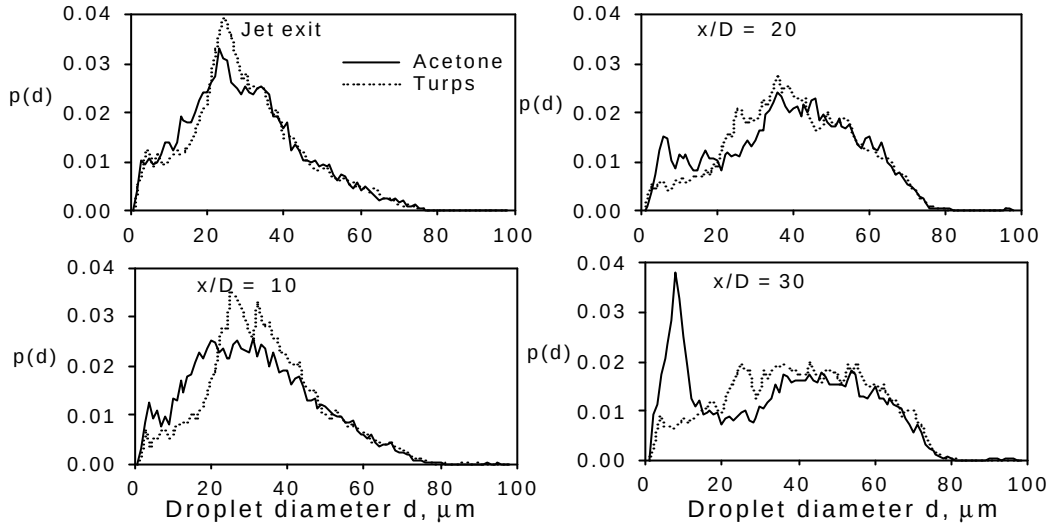

Figure 2. Probability density functions of droplet size on the centreline.

distance, the evaporating acetone pdf shows a growing peak at around 10 µm, a feature absent in the pdf's for non-evaporating turps. At x/D = 30, the acetone pdf has become distinctly bimodal on the centreline, and p(d) at 20 - 40 µm is reduced. To the authors' knowledge, this feature has not been reported elsewhere, and merits detailed examination.

Although it is known [8] that the size distribution produced by ultrasonic nebulizers is approximately lognormal, it is noteworthy that the jet exit pdf's in Figure 2 do not have this distribution. The manner of entrainment into the carrier flow and the transit history in the nozzle tube are thought to be the main causes of the modified pdf's, which are clearly much less skewed towards small droplet diameters than the lognormal distribution.

3.1 Flow Fields

The velocity and turbulence fields for both the acetone and mineral turpentine spray jets are found to be similar except at the jet exit plane where the evaporation of acetone reduces the temperature. Therefore at x=0, the mean axial velocity of the acetone jets is about 4-5% lower only for the smallest size class droplets (d<10 µm). With this qualification, and to avoid repetition, data for the acetone jets only are presented in this section.

Figure 3 shows radial profiles of mean axial velocity U, and rms velocity variation, u', for the acetone spray only. The abscissa is normalized by the velocity half-radius, L_u , which is the radius at which the excess mean velocity, $U-U_{coflow}$, is one half of the centreline maximum. It is seen that slip velocities at the jet exit are negative for the large droplets due to their greater inertia in accelerating from rest in the 200 mm long mixing tube. Beyond the jet exit, the slip velocities are reversed as the gas phase now has a braking effect on the droplets. The centreline decay of mean axial velocity for acetone and turps is virtually identical, with the expected asymptote to the -1 slope for the gas phase, as approximated here by the small droplet size class (d<10 µm).

In the shear layer, small droplets have the largest rms velocity, and the large droplets the lowest rms, indicating that the shear-generated turbulence has less effect on large droplets. It is in a sense misleading to speak of "turbulence rms" in relation to large droplets that interact more weakly with the gas phase, since the local velocity variation is to some extent a residue of droplet trajectory and velocity differences at the jet exit. The expected ratio of radial to

axial rms turbulence of around 0.7 for a classical round jet is found for the small droplets in both these sprays (not shown here). This ratio decreases rapidly with increasing droplet size, as the larger drops largely retain their trajectories and initial range of streamwise velocity whilst the production of radial velocity fluctuation, v', is low due to the weak interaction between large particles and the gas phase.

The Reynolds stress, u'v', (obtained by separate measurements with both velocity components as well as size recorded) shows peaks in mid shear layer, with lowest values for the largest droplets. However, the correlation coefficient, R_{uv}, shows the opposite trend, with the smallest range approximating to the usual gas phase values with a peak around 0.5, and larger sizes reaching higher peak values, up to 0.7. Hardalupas *et al.* [9] argue that the strong correlation is explained by history effects, i.e., the fanning-out of large droplets with initial high momentum.

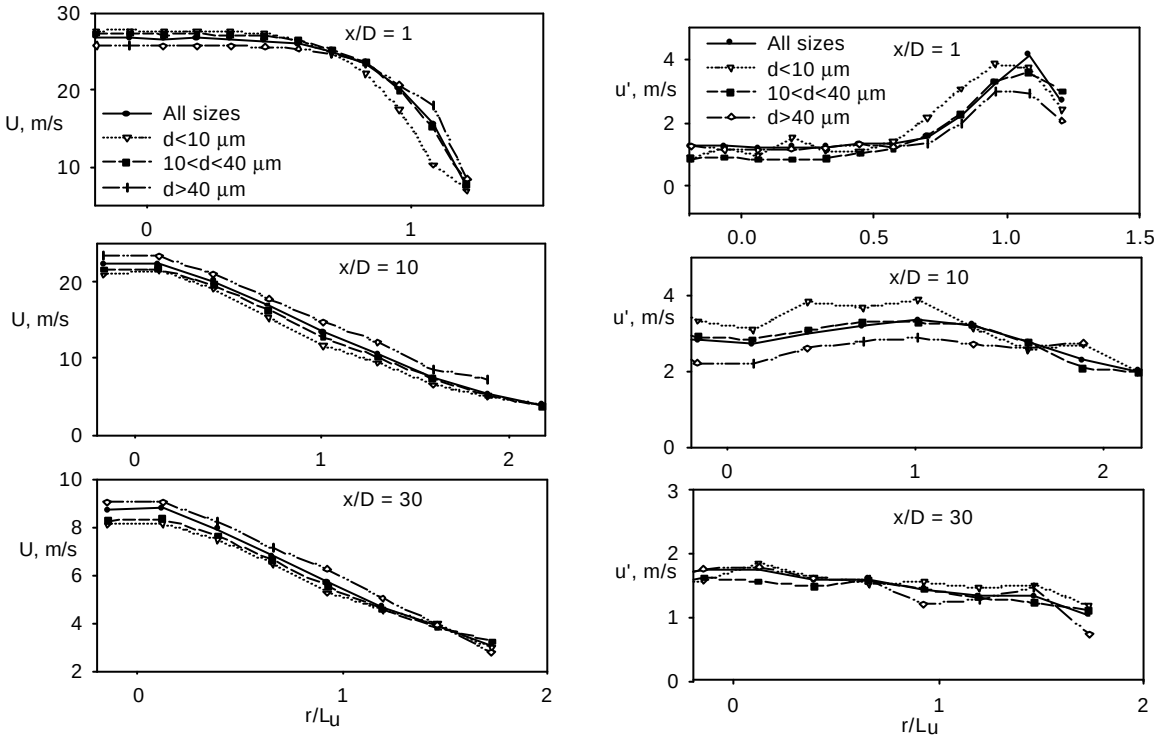

Figure 3. Development of axial mean (U) and rms (u') velocity for the acetone jet

3.2 The droplet fields

The decay of acetone and turps droplet volume fraction, V_f, on the axis, shown in Figure 4, proceeds inversely with droplet size, consistent with turbulent diffusion being the main mechanism for the radial transport of the dispersed phase. However, the most noteworthy feature is the persistence, in the acetone case, of high axis values in the size class <10 μm at x/D = 20 to 30. By contrast, in the turps case, V_f decays smoothly for all size classes. This is consistent with the observed size distributions in Figure 2.

Plots of half-radii are shown in Figure 5 for both gas phase excess velocity and droplet volume fraction. (The half radii are defined as in Section 3.1). The velocity is taken as the

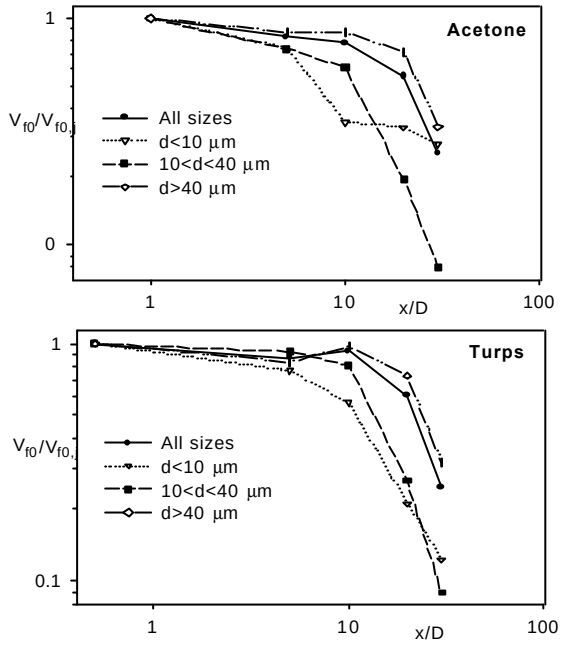

Figure 4. Centreline decay of volume fraction, V_{f0}, normalized by its value at the jet exit.

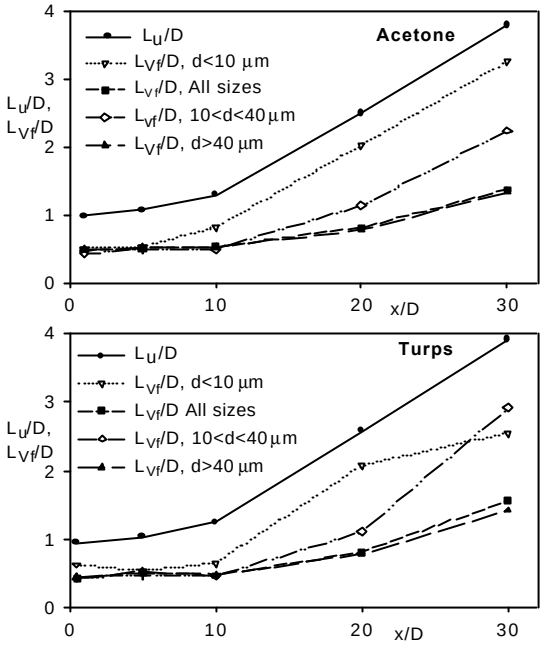

Figure 5. Axial variation of half-radii of velocity, L_u, and droplet volume fraction, L_{Vf}.

velocity of the d<10 μm droplet size range. The profiles shown in Fig. 5 illustrate the difference between turbulent momentum transport and liquid (or droplet) transport. Whilst the distribution of U at the jet exit (as seen in Figure 3) is almost a top-hat profile with

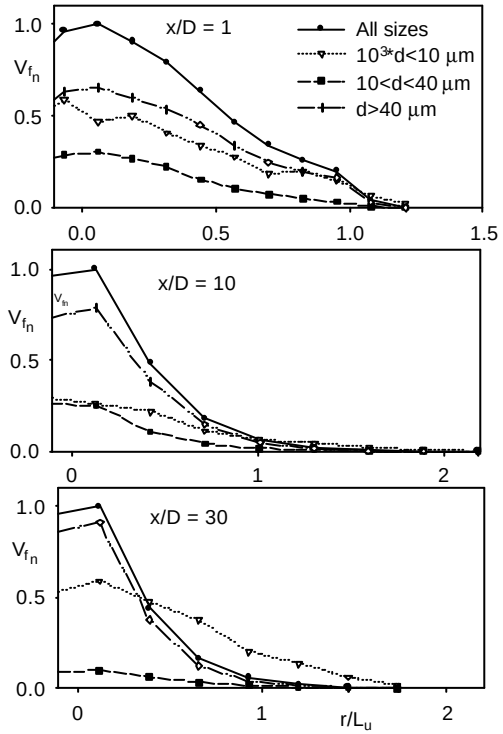

Figure 6. Acetone jet. Radial profiles of mean droplet volume fraction V_f, normalized by axis value of V_f for all sizes.

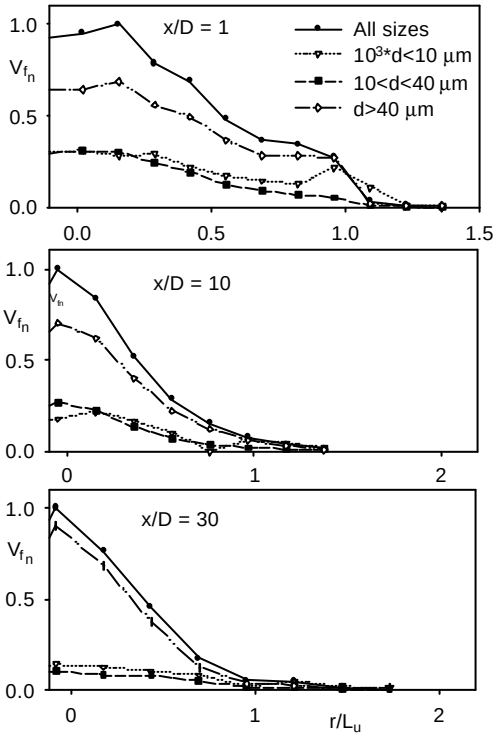

Figure 7.Turps jet. Radial profiles of mean droplet volume fraction V_f, normalized by axis value of V_f for all sizes.

Lu/D=1, the droplet distribution is closer to Gaussian, with L_{Vf} around 0.5D (Figure 5). The low dispersion of large droplets reflects the weak interaction with the gas phase turbulence. A comparison of acetone and turps data indicates that the half-radii are little affected by the evaporation rate, to within the measurement uncertainty. (The rather low value of L_{Vf} in the turps case at x/D=30 and d<10 μm may be an anomaly due to low data rate at this condition.)

In Figures 6 and 7, radial profiles of mean droplet volume fraction are compared for the acetone and turps sprays. As mentioned earlier, the high initial concentration on the centreline produces initial half-radii much smaller than for momentum; the downstream data need to be qualified by this fact. The marked increase in volume fraction for the smallest acetone droplets at x/D=30 is again seen to be consistent with the pdf's of droplet distribution.

Droplet flow rates, obtained by integration of measured fluxes across the jet at each x/D, are shown in Figure 8. It is seen that the overall turps flow rate ("All sizes") is well conserved; we view the 3 per cent fluctuation from the mean as measurement noise. When the results are split into size classes, the turps flow rates show greater variability, without clear trend. By contrast, the acetone case is clearer, with near zero evaporation for the largest size range, whilst smaller droplets evaporate more rapidly. However, there is rapid initial loss for d<10 μm, and then a remarkably large increase in flux beyond x/D=10. This increase is in qualitative agreement with the development of droplet pdf's in Figure 2.

As it can readily be shown that the size distribution and low number densities in this spray exclude droplet breakup and agglomeration, the variation in flow rates here is attributed to evaporation alone. The fact that only the acetone, and not the turps spray, shows the increased downstream flux for d<10 μm, despite similar jet exit distributions (Figure 2), strengthens the argument that this is not an artifact. In addition, the measurements were all made with instrument settings and other conditions unaltered, and were later repeated for confirmation. To account for this behaviour, it may be surmised that the large slip velocities documented in Figure 3 cause medium- and large size droplets to evaporate rapidly until they reach the size range d<10 μm, where the slip becomes unimportant, so that an accumulation of droplets occurs in this range [6]. However, given that there must always remain uncertainties associated with instrumentation as sophisticated as the PDPA system, this aspect of the results need to be viewed with caution until independently substantiated by experiments or modelling.

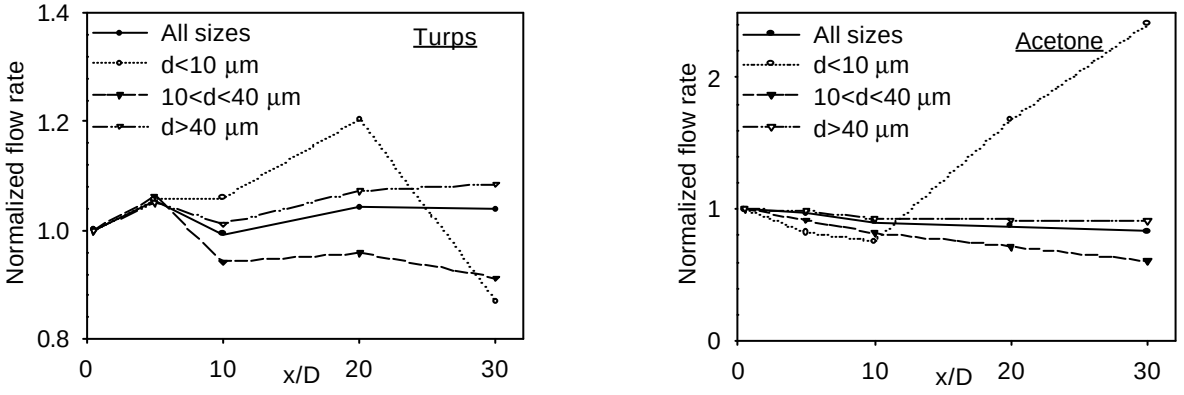

Figure 8. Total droplet flow rates, normalized by values at the jet exit.

Concluding remarks

These results reveal a simple, well-behaved classical turbulent jet flow, where accurate droplet flux measurements have been demonstrated by conservation of the overall flow rate in the non-evaporating case. There is strong turbulent diffusion of small droplets, with the largest droplets confined to trajectories with low dispersion, positive slip velocity and high ratio of axial to radial rms turbulence velocity. The size distribution probability density functions (pdf's) for the non-evaporating spray change only modestly with downstream distance. The acetone spray pdf's, however, show distinct shifting of peak values towards smaller sizes, with a distinctly bimodal shape developing at distances of 10 to 30 jet diameters from the exit. Measured fluxes of the dispersed phase also show a large downstream increase in the flux of droplets in the 5-15 micron range, consistent with the observed bimodal pdf's for the acetone case.

Acknowledgment

This work is supported by a grant from the Australian Research Council.

References

[1] Masri, A R, Dibble, R W and Barlow, R S 1996 *Prog. Energy Combust. Sci.* **22** 307-362
[2] CHEN Y-C, Stårner S H and Masri, A R 2002 *14th Australasian Fluid Mechanics Conference*, Adelaide University, Adelaide, Australia, Dec 10-14.
[3] CHEN Y-C, Stårner, S H and Masri, A R *Twenty-ninth Symposium (International) on Combustion, The Combustion Institute* (in press).
[4] Ferrand V, Bazile R and Boree J 2001 *Experiments in Fluids* **31** 597-607
[5] Kennedy I M and Moody H M 1998 *Experimental Thermal and Fluid Science* **18** 11-26.
[6] Nijdam J J, Stårner S H and Langrish T A G 2003 *Experiments in Fluids* (under review).
[7] McDonnell, V G and Samuelsen, G S 1993 *Atomization and Sprays* **3** 321-364
[8] Dumouchel C, Sindayihebura D and Bolle L 2002 *Proc of ILASS-Europe Conf. Zaragoza, Spain, Sept 9-11*
[9] Hardalupas Y, Taylor A M K P and Whitelaw J H 1989 *Proc R. Soc. Lond A* **426** 31-78
[10] Rüger M, Hohmann S, Sommerfeld M and Kohnen G 2000 *Atomization and Sprays* **10** 47-81